WHICH HAND? TREMOR AVERAGE AREA AND PEAKS

ELEN4012A – EIE Investigation 2022 – Jesse van der Merwe (1829172)

School of Electrical & Information Engineering, University of the Witwatersrand, Private Bag 3, 2050, Johannesburg, South Africa

Abstract: This investigation focuses on the development and implementation of two methods used to produce a tremor severity rating that measures the tremor reduction after Focused Ultrasound Treatment on a patient's treated and untreated hand. This is to attempt to quantitatively determine whether the treatment is successful using image processing and computational analysis. This would remove the need for an expert physician and provide a more accurate and less biased result. This paper focuses on image pre-processing, as well as methods 2A (average area) and 2B (peak-trough distances. The results show that these methods reliably indicate the success of the treatment overall and per patient by using the tremor severity ratings to determine whether the tremor has decreased in either hand.

1. INTRODUCTION

Focused Ultrasound Treatment is used to treat Parkinson's disease and essential tremor. This investigation aims at quantitatively investigating the efficacy of this treatment using computational and statistical analysis of spiral drawings. The aim is to provide insight about the extent that these results can be used to assess the severity of the tremor on the patient's treated vs untreated side after the treatment. This will help determine whether the treatment is successful in reducing the tremor or slowing the progression of the disease without the need for a medical practitioner with potential bias. This document details the various methods investigated and developed, including the pre-processing of the provided template data, as well as the analysis of the data and resulting quantitative values.

2. LITERATURE SURVEY

2.1. Focused Ultrasound Treatment

Focused Ultrasound Treatment (FUS) is a new and promising non-invasive treatment for movement disorders that cause involuntary rhythmic movements of body segments. Two such disorders, that produce similar symptoms, include Parkinson's disease (PD) and essential tremor (ET). Sound waves, which contain acoustic energy, are delivered through the physical barrier of the brain to create lesions on targeted brain tissue [1]. By creating these lesions on the part of the patient's brain responsible for the communication of sensory and motor signals, abnormal brain activity is interrupted, which reduces uncontrollable movements with immediate effect [1]. This reduces the unwanted tremor caused by PD or ET. This is a unilateral treatment since FUS is only performed on one side of the brain (usually on the dominant hand side [2]). This treatment shows immediate reduction in tremor on the treated side of the body.

2.2. Hand-drawn Shapes

The observational analysis of hand-drawn shapes by a neurologist is widely used as a severity test of movement disorders [3]. Analysis of handwriting is avoided due to stylistic differences skewing the test results [4]. An Archimedes spiral is often used as it captures the frequency, amplitude, and direction of a tremor [4]. Long,

straight, line drawings offer similar results. These drawings require one continuous pen motion and thus they are able to emphasise the abnormal movements specific to movement disorders [4]. The typical characteristics of tremor types can be found in [[4], Tab. 1]. This table shows that ET and PD have similar characteristics, however, previous studies have shown that computational analysis of such drawings can reliably discriminate between ET and PD [3]. Further, the combination of traditional and computational analysis has provided significant progress in the classification of disease severity [5].

2.3. Existing Methods

Analysis of patterns in tremor diagnosis spiral drawings for automated classification [6]: This method focuses on finding the relative orientation of all pixels in a hand drawn Archimedes' Spiral. This approach is insensitive to drawing errors and produces accurate results. This approach is the basis for method 1 of this project.

Application of machine learning and numerical analysis to classify tremor in patients affected with essential tremor or Parkinson's disease [7]: Three methods try to match the qualitative clinical tremor ratings. 1) Digital pen spiral tracing analysis. 2) Analysis of a gyroscopic 'Shimmer' device data using RMS methods. 3) Analysis of the 'Shimmer' device data using machine learning decision tree algorithm. These methods matched the clinical tremor rating 78%, 42% and 82% respectively.

Quantification of tremor with a digitizing tablet [8]: Using a commercially available digitizing tablet, the tremor introduced by drawing an Archimedes spiral or writing words can be analysed. The quantification includes acceleration, peak-to-peak amplitude, velocity, power, and displacement. This approach is the basis for method 2 of the project, without the luxury of a digitizing tablet.

Quantification of the drawing of an Archimedes spiral through the analysis of its digitized picture [9]: Spirals are analysed after reconstructing the temporal sequence of an Archimedes spiral drawing. Method 1) Cross-correlation coefficient with spiral template. Method 2) Mean and standard deviation of distance between each point of the spiral drawing and the corresponding point of the model. Method 3) Fourier Transform of reconstructed spiral.

3. PROJECT PLAN

At the commencement of this project, the submitted investigation Project Plan, found in Appendix 3, was discussed with Professor Aharonson, the supervisor of this project. It was quickly realised that the plan did not correctly cover the scope or complexity; no machine learning would be required, since image processing and computational analysis would be enough to answer the investigation question. Thus, a new project plan, scope and schedule was created. The corrected Gantt chart can be found in Appendix 7.

4. DATA

4.1. Database access and ethical clearance

Fully anonymised data of patients with either PD or ET was provided by the Rambam Medical Centre, Haifa Israel. Permission to use this data was subject to the obtainment of ethical clearance from the University of Witwatersrand. The Clearance Certificate for this project as well as the permission letter from Dr Schlesinger can be found in Appendices 5 and 6 respectively.

4.2. Patients

Out of the 122 patients, 34 are undergoing treatment for PD, and the remaining 88 for ET. This investigation does not require any differentiation between diseases, but rather whether the tremor is reducing, and treatment is working.

4.3. Data

The database consists of templates that are filled in with both the treated and untreated hands before and after receiving treatment. Each patient uses a pen to physically fill in a template. This is then scanned and saved as a PDF. Each template consists of two Archimedean spiral drawings (spiral A and spiral B), and multiple straight-line drawings (line-block C) as shown in figure 1A.

5. PRE-PROCESSING OF DATA

5.1. Original Spiral Isolation Code

Kelvin da Santos developed a pre-processing python script specifically for isolating the spirals for his master's research [10]. After meeting with him, permission was granted to use and further improve this code to better suit the needs of this project. His code is based on the 'OpenCV Text Detection (EAST text detector)' article by Adrian Rosebrock [11] which makes use of a text detector library to detect the labels "Drawing A", "Drawing B" and "Drawing C". This returns the four coordinates of each corner of these text areas, saved in a list. This process can be seen in figure 1B. From here, the width of each spiral was approximated using the start positions of "Drawing A" and "Drawing B". Finally, using crop tolerance values and further manipulation, each of the two spirals were cropped and saved as new images – as seen in figure 1C.
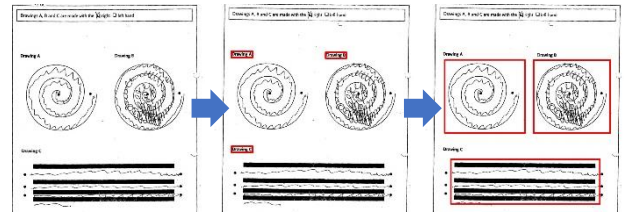

Figure 1: A) Original filled in template, B) text detection and C) image isolation and cropping procedure.

5.2. Improvement of Isolation Code

Too many incorrectly cropped spirals: Most of the scanned drawings are pixelated, slightly rotated, or contain erroneous pen or other markings. This causes the text detection code to sometimes incorrectly identify erroneous markings as text, which leads to inaccurately cropped spirals. This further causes the results of the image analysis to become skewed due to extreme data outliers. Since there are 122 patients, with each patient having anywhere between 2 and 20 scanned drawing, it was imperative to correct these inaccurately cropped spirals within the code. Thus, much time was spent improving the pre-processing code by adding more error detection and correction before the spirals were cropped. It is imperative that as many spirals and line-drawings are isolated and accurately cropped to have as much useable data as possible.

Missing line-drawing C: This code did not extract the line-block C section of the templates. Thus, it was expanded to do so, since methods 2A and 2B require this line drawing.

Performing logic checks: To reduce the erroneous cropping, more logic checks were implemented. This included deciding whether the coordinates of the detected text matches the approximate expected positions of the text. Other detected text can be safely ignored since there should only be three sets of coordinates.

Not only relying on "Drawing A": The previous method implemented in the code relied on the position of "Drawing A" to determine both the width of the spirals and the cropping position of both spirals. However, in some instances, the "Drawing A" text was not detected, and thus the entire process would fail. To prevent this from happening, a combination of all the relative positions of any available detected text is used to ensure the best possible cropping positions. If no text is detected, average values are used instead.

Final cropped images: The cropped spiral A, spiral B, and line-block C for each scanned drawing of every patient is saved as a JPEG image. Each of these final images are converted to greyscale and resized to ensure consistent pixel distribution. The spirals are saved as 300×300 pixel images, and the line-blocks as 600×300 pixel images. This allows for more accurate comparison further since every image is exactly the same size regardless of the image quality of the original scanned template.

5.3. Extraction of line-drawing C from line-block C

The line-block C for each scanned drawing had already been extracted. It was decided that only the top-most line-drawing of each line-block would be required as it is the largest line and provides the most space for patients to draw. Method 2, mentioned in section 7 below, analyses this line-drawing. Extracting only the line prevents the large black rectangles from influencing the image processing and analysis techniques. There is an overall rotation in many of the templates caused by human error whilst scanning. Thus, once the black rectangles are identified, compensation for this rotation needs to occur to prevent erroneously cropped lines.

Rectangle rotation correction: Using code snippets from the article "Cropping Rotated Rectangles from Image with OpenCV" by jdhao [12], as well as the article "OpenCV shape detection" by Adrian Rosebrock [13], the coordinates of each of the detected black rectangles were saved in a list. This list is then sorted to ensure the coordinates are in a standard order: top-left, top-right, bottom-right, bottom-left. The only two rectangles needed are the top two, as these can then be used to approximate the coordinates of the line drawing that is positioned in between these rectangles. The first rectangle's bottom coordinates become the line-drawing's top coordinates. The second rectangle's top coordinates become the line-drawing's bottom coordinates. With these new coordinates, the $getPerspectiveTransform()$ function from the OpenCV Python package is used in conjunction with the $warpPerspective()$ function to produce a straightened line-image. A small number of pixels is then removed from each side of the new image to ensure that no remnants from the black rectangles persist. A brief logic check of whether the width is indeed larger than the height ensures the rotation of the rectangle is correct and makes an appropriate correction if it is not. This image is then saved as a JPEG. This process is summarised in figure 2.
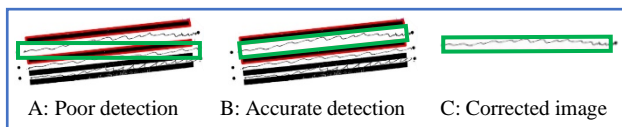

| A: Poor detection | B: Accurate detection | C: Corrected image |

Figure 2: Rectangle detection and rotation correction process

Final extracted singular lines: The main goal of this pre-processing section is to successfully extract as many possible line-drawings as possible, with high precision and very little error. Out of the 1161 total scanned images, a total of 1018 line-drawing images were successfully extracted. This is a success rate of 87.8%. After further analysis, it was realised that most of the unsuccessful extractions were due to the fact that a handful of patients did not fill in the line-block C part of the template at all. Thus, the success rate of line-drawing extraction is even higher, and sufficient for this project.

6. METHOD 1: EDGE ANGLE SPIRAL ANALYSIS

The spiral drawings on each template were analysed using a method researched and implemented by group member, Robyn Gebbie [14]. This chosen method and subsequent results will be briefly discussed to allow for a final comparison and conclusion to be drawn.

6.1. Method

Edge angles: Sobel edge detection filters are used to find the horizontal and vertical gradients of each pixel. The orientation ('edge angle') of each pixel is then found by taking the inverse tangent of the ratio of the gradients [15].
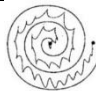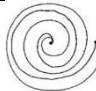
Pixel angles: The centre of each spiral is calculated. The ratio of the vertical and horizontal distances between the centre and each pixel is then found to take the inverse tangent and produce the 'pixel angle' [6].

Relative orientation: The relative orientation is found by subtracting the pixel angle from the edge angle for each pixel. This is plotted as a histogram. A high standard deviation of the data indicates a worse tremor. Further, a wide distribution of angles indicates a larger variety of angles and thus a worse tremor. A higher frequency of edge angles also indicates a worse tremor. The normalised standard deviation is found for every spiral of each patient to allow for comparison between patient's own hands, as well as between patients in general.

6.2. Results

Two spirals, as seen in table 1, are used to demonstrate this method. Spiral A1 has a higher normalised standard deviation than spiral A2. The histogram in figure 3 also shows that spiral A1 has a higher frequency of the edge angles. This correctly indicates that spiral A1 has a worse tremor compared to spiral A2.

Table 1: Spiral A1 &A2 image and normalised standard deviation

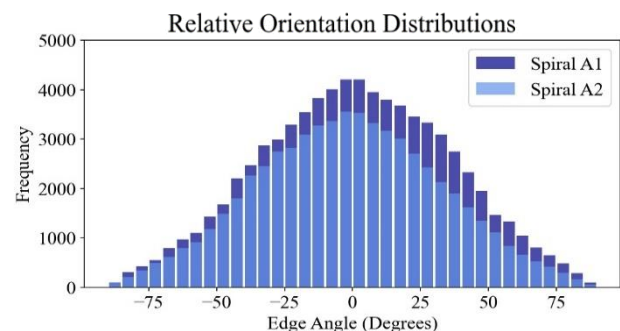|	Spiral A1: Before treatment	Spiral A2: 1 month after treatment
Extracted spiral image		
Normalised standard deviation	0.64	0.15

Figure 3: Relative orientation distributions of spirals A1 and A2

7. METHOD 2: AVERAGE AREA AND PEAKS

After the pre-processing mentioned in section 5.3 above, each of the top-most line drawings has been successfully extracted for each patient's scanned drawings. These will be referred to as 'the line(s)'. There are a total of 1018 useable lines that were extracted and saved as JPEG images. This method relies on converting the line into a python list, on which analysis can be made.

7.1. What can be extracted from a line?

If a patient has a severe tremor, it is extremely difficult for them to draw a straight line. Through observation, it was noted that the number of peaks is an indication of the frequency – and thus the severity – of the patient's tremor. In general, the more peaks indicate a worse tremor. Furthermore, the distance between each adjacent peak and trough provide another indication of the severity of the tremor. However, a larger distance generally only indicates a worse tremor when occurring with a high number of peaks. With this in mind it was decided to calculate the average area under the line, as well as the number of peaks and peak-trough distance for each line. This can easily be achieved in Python using the various mathematical packages. However, first a line function (in the form of a list) must be extracted from the line itself.

7.2. Determining the line function

Table 2: Patient #5's treated hand: Extracted line images

| BEFORE | ~~~~~~~~~ |
| AFTER 1 YEAR | ~~~~~~~~~ |

Line noise reduction: Many of the lines still contained erroneous pixel markings that needed to be removed. Pixelation and blurriness due to the poor quality of each scan also needed to be reduced. This will allow for higher-quality analysis. First, each line is converted to grayscale. Then, using the $point()$ function from the PIL.Image Python package [16], the colour of each pixel above a particular greyscale value threshold is mapped to black. All other pixels are mapped to while. This allows any grey erroneous pixels to be removed. Further, this leaves only the required pixels, which are now guaranteed to be black. The result of this process can be seen in table 2.

Converting to function: Using the NumPy Python package's $argwhere()$ function [17], the indices of pixels that are black in colour are read into a multidimensional array. The x- and y-coordinates of each index is then extracted, which successfully creates two arrays of corresponding coordinates for the x- and y-values of each pixel found in the line. By sorting these according to the x-values, these arrays can easily be plotted on a graph. These arrays will be referred to as the 'line function'. For easier analysis, each graph is shifted down by the average y-value so that it is centred around the x-axis. It can quickly be seen that these points are extremely scattered and noisy, with hundreds of peaks and troughs, as seen in figure 4A.

Graph noise reduction: To reduce the noise of the resulting graphs, the real one-dimensional Fourier Transform $rfft()$ is computed using the SciPy.fft Python package [18]. All entries in the y-value array are real which means the faster and more optimized $rfft()$ can be used. As seen in the example in figure 4B, there is only a small range of useful frequencies present. Only the bottom 5% of the frequencies are kept, and the higher, unwanted frequencies caused by the pixelated/blurry input are discarded. The inverse real discrete Fourier Transform is then applied, resulting in noise-free line-graphs, as seen in figure 4C.

Extreme frequency bug fix: It should be noted that some of the line-graphs produced an extreme range of frequencies. An example of this can be seen in figure 4A; the right graph has a much smaller range of y-values and yet considerably more erroneous noise-induced peaks compared to the left graph. Keeping 5% of the frequencies in this example did not reduce the noise sufficiently. To fix this error the graph noise reduction process was repeated until sufficient noise reduction had occurred. It was known when this point was reached when the number of peaks is accurate to the line itself and not due to noisy plotting.

7.3. Method 2A: Average Area Under Line Function

Once the line function had been successfully determined, the NumPy Python package's $trapz()$ function [17] is used to calculate the total area under the absolute value of the line function. However, it was quickly realised that if the line was drawn slanted then this total area would be exaggerated, regardless of tremor. Thus, it was decided to find the average area of small segments along the line. This provided a more reliable tremor severity rating and helped to reduce the impact of slanted lines.

7.4. Method 2B: Average Peaks × Peak-Trough Distance

The SciPy.signal Python package's $find\_peaks()$ formula [18] was used to calculate the total number of peaks and troughs within the line function, as well as the coordinate positions of each. From here these values are iterated through to calculate the distance between each peak and adjacent trough(s). Finally, the average peak-trough distance value is found. Since a larger average peak-trough distance generally only indicates a worse tremor when occurring with a high number of peaks, the two values are proportionally linked to the severity of the patient's tremor. Thus, the product of these two values is used as the indication of tremor severity for method 2B.

7.5. Additional Values

Some additional values were calculated for each line; including the standard deviation of both the total and average areas, the maximum value of the line function as well as the maximum frequency of each line function's Fourier Transform. This can be seen in table 3. These values were not analysed due to time constraints of the project.

7.6. Results

The results from two chosen lines will be used to demonstrate the validity of this method. Patient 5 was chosen since there is significant improvement between the lines drawn by their treated hand before receiving treatment and 1 year after treatment. These two lines will be referred to as the 'before-line' and '1-year-line'. These line images can be seen in table 2 above, with the processes behind methods 2A and 2B shown in figure 4A-E. Table 3 shows the final calculated values. The values for the before-line are higher than the 1-year-line in all instances. However, as mentioned above, only the values required for methods 2A and 2B are focused on in this report.
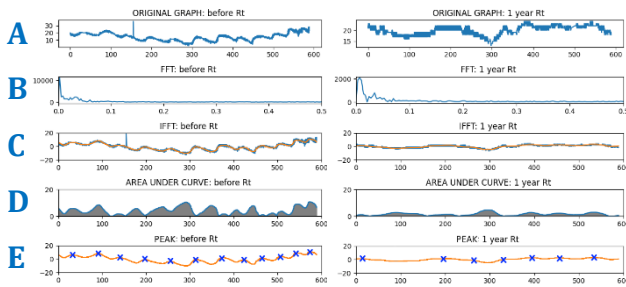

Figure 4: Noise reduction and analysis stages for method 2A& 2B

Table 3: Calculated values from the line function of patient #5's treated hand before and 1 year after treatment

Calculated Value from Line Function	Before	1 year
Total area ($pixels^2$)	15442.10	4316.75
Standard deviation of total area	5.52	2.10
Maximum value ($pixels$)	21.42	4.17
Maximum frequency (Hz)	11087.03	2093.07
METHOD 2A: Average area ($pixels^2$)	**13.44**	**0.86**
Standard deviation of average area	122.74	51.09
Number of peaks	12	7
Average peak-trough distance ($pixels$)	5.81	2.43
Num. Peaks × Avg. Peak-Trough Distance (METHOD 2B)	**69.67**	**17.02**

7.7. Future Improvements

Slanted lines: With method 2B, a result of a large peak-trough distance coupled with a very low number of peaks was often an indication of a slanted line image. Likewise, with method 2A, an incorrectly large average area was often an indication of a slanted line. More advanced pre-processing could be developed to straighten the lines as much as possible. However, first, research should be performed and/or medical professionals consulted, to determine whether a slanted line is an indication of a worse tremor. This would mean that such slanted lines are valuable and should not be corrected.

Additional values: As mentioned above, the four additional values calculated for each line should be analysed to determine whether they provide further insight. Further research in the frequency domain should be conducted as it is a powerful tool that could provide interesting and unique insights.

8. OVERALL DISCUSSION OF RESULTS

Various tremor severity ratings were determined for each patient's treated and untreated hand over various time periods. Method 1 uses the normalised standard deviations of the relative orientation distributions of spiral A. Method 2A uses the average area under the line C. Method 2B uses the product of the number of peaks and average peak-trough distance of line C. To determine whether these methods are effective indications of the treatment's success, the average tremor severity rating, as well as percentage of patients whose tremor improved, was determined. These graphs can be seen in figures 5-7. Full sized versions can be found in Appendix 9.

Tremor severity: There is an immediate decrease in the average tremor severity of the treated hand in all methods. This indicates that the treatment is successful. Further research should be conducted to determine whether these values reflect the medial diagnosis of each patient. Interestingly, both methods 2A and 2B demonstrate a decrease in the tremor severity of the untreated hand as well. This should be further analysed to determine whether it is accurate or a flaw of these particular methods.

Percentage of improved patients: Table 4 shows the average percentage of how many of patients improved after treatment over time. Methods 1 and 2B have very similar averages which indicates that the FUS treatment successfully reduces the tremor in the treated hand. Method 2A has a lower average. Further investigation should be conduction to determine which method most accurately reflects the medical diagnosis of each patient.

Amount of data of later years: As indicated by the red lines in figures 5-7, the number of patients with data for later years drastically decreases. This affects the reliability of these years' results due to insufficient data.
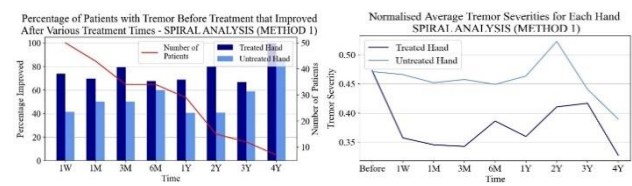

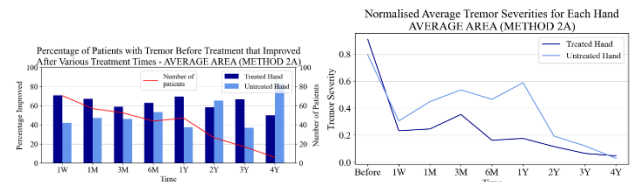Figure 5: Results of method 1 – spiral analysis

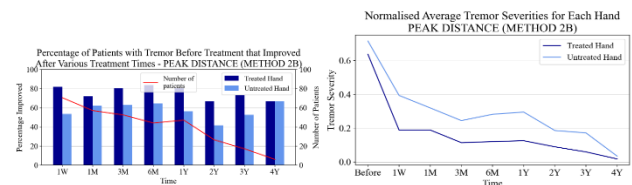Figure 6: Results of method 2A – average area

Figure 7: Results of method 2B – peak-trough distance

Table 4: Average percentage of improved patients according to each method implemented

% Improvement of Patients	Method 1	Method 2A	Method 2B
TREATED HAND	75.8%	63.5%	75.7%
NON-TREATED HAND	53.4	51.4%	57.4%

9. FUTURE IMPROVEMENTS

Bringing in an Expert Physician: The accuracy of these implemented methods should be evaluated by an expert physician or medical processional in order to truly determine whether the results are accurate and reliable enough to be used in the medical field.

Combing methods: Research should be conducted to determine whether combining the results of all methods would produce a more reliable result and/or whether methods 2A and 2B can be applied to the spiral images. This would allow for additional comparative opportunities to further validate the results of methods 2A and 2B.

AI and Machine Learning: The above computed data can be compiled with existing patient information – such as age, medical history, dominant hand etc. This would allow for a machine learning model to be developed to potentially predict whether a patient would have successful treatment, or even how much improvement would be achieved in each hand. This would be invaluable to the medical physicians and specialists and the patients themselves who are opting into this relatively new FUS treatment.

Pathological vs Physiological Tremor: Further research should be conducted into whether these methods can accurately detect physiological tremor (peak-trough distance of less than 0.5mm which occurss in normal persons [8]) or whether it only can detect mild pathological tremor (peak-trough distance of greater than 1mm which impairs a patient's function [8]). This would determine whether control groups can be analysed to better provide training data for potential machine learning applications.

10. CONCLUSION

The implemented methods reliably produce three different tremor severity ratings. These can be used to determine which of a patient's hand had been treated, whether the treatment was successful, and the amount by which the tremor was reduced in either hand. This points to the potential of using such methods as non-biased evaluation tools of the treatment's efficacy, without needing to involve an expert physician's observation. However, there are plenty of improvements to be made, and further validation of the results is required.

11. REFERENCES

[1] H. Baek, D. Lockwood, E. J. Mason, E. Obusez, M. Poturalski, R. Rammo, S. J. Nagel and S. E. Jones, "Clinical Intervention Using Focused Ultrasound (FUS) Stimulation of the Brain in Diverse Neurological Disorders," *Frontiers in Neurology,* vol. 13, 2022.

[2] M. Rohani and A. Fasano, "Focused Ultrasound for Essential Tremor: Review of the Evidence and Discussion of Current Hurdles.," *Tremor and Other Hyperkinet Movements (NY),* vol. 462, no. 7, 2017.

[3] N. Seedat, V. Aharonson and I. Schlesinger, "Automated machine vision enabled detection of movement disorders from hand drawn spirals," *2020 IEEE International Conference on Healthcare Informatics (ICHI),* pp. 1-5, 2020.

[4] J. Alty, J. Cosgrove, D. Thorpe and P. Kempster, "How to use pen and paper tasks to aid tremor diagnosis in the clinic," *Pract Neurol,* vol. 17, pp. 456-463, 2017.

[5] V. Aharonson, N. Seedat, S. Israeli-Korn, S. Hassin-Baer, M. Postema and G. Yahalom, "Automated stage discrimination of Parkinson's disease," *BIO Integration,* vol. 1, no. 2, pp. 55-63, 2020.

[6] A. Wille, M. Sangaré and S. Winter, "Analysis of Patterns in Tremor Diagnosis Spiral Drawings for Automated Classification," Institut für Neuroinformatik, Ruhr-Universität Bochum, Germany, Bochum, 2013.

[7] S. Aktar, H.-Y. Tseng, P. Barthelmess, P. R. Cohen, N. D. Darnall, K. C. Donovan and D. C. Lin, "Application of machine learning and numerical analysis to classify tremor in patients affected with essential tremor or Parkinson's disease," *Gerontechnology,* vol. 10, no. 4, pp. 208-219, 2012.

[8] R. J. Elble, R. Sinha and C. Higgins, "Quantification of tremor with a digitizing tablet," *Journal of Neroscience Methods,* vol. 32, pp. 193-198, 1990.

[9] F. Miralles, S. Tarongí and A. Espino, "Quantification of the drawing of an Archimedes spiral through the analysis of its digitized picture," *Journal of Neroscience Methods,* vol. 152, pp. 18-31, 2006.

[10] K. da Silva, "Tremor Classification," 7 September 2020. [Online]. Available: https://github.com/kdasilva835842/tremor_classification. [Accessed 29 September 2022].

[11] A. Rosebrock, "OpenCV Text Detection (EAST text detector) - PyImageSearch," PyImageSearch, 20 August 2018. [Online]. Available: https://pyimagesearch.com/2018/08/20/opencv-text-detection-east-text-detector/. [Accessed 16 July 2022].

[12] jdhao, "Cropping Rotated Rectangles from Image with OpenCV," jdhao's digital space, 23 February 2019. [Online]. Available: https://jdhao.github.io/2019/02/23/crop_rotated_rectangle_opencv/. [Accessed 26 July 2022].

[13] A. Rosebrock, "OpenCV shape detection - PyImageSearch," PyImageSearch, 8 February 2016. [Online]. Available: https://pyimagesearch.com/2016/02/08/opencv-shape-detection/. [Accessed 20 July 2022].

[14] R. Gebbie, "Analysis of the Effect of Focused Ultrasound Treatment on Hand Tremor: Quantification of Tremor in Spiral Drawings," 4th Year Investigation Report 22G05, School of Electrical and Information Engineering, University of the Witwatersrand, Johannesburg, 2022.

[15] P. Delmas, "Edge Detection," in *COMPSCI 373 Semester 1*, Auckland, The University of Auckland, 2010, pp. 40-51.

[16] Alex Clark and Contributors, "Image Module - Pillow (PIL Fork) 9.3.0 documentation," pillow, 2022. [Online]. Available: https://pillow.readthedocs.io/en/stable/reference/Image.html. [Accessed 6 September 2022].

[17] NumPy Developers, "NumPy documentation - NumPy v1.23 Manual," NumPy, 2022. [Online]. Available: https://numpy.org/doc/stable/index.html. [Accessed 5 September 2022].

[18] The SciPy community, "SciPy documentation - SciPy v1.9.3 Manual," SciPy, 2022. [Online]. Available: https://docs.scipy.org/doc/scipy/index.html. [Accessed 9 September 2022].